Velocity Perturbation Distributions in the Breakup of Artificial Satellites

Gautam D. Badhwar* and Arjun Tan†
NASA Johnson Space Center, Houston, Texas
and
Robert C. Reynolds*
Lockheed Engineering & Science Company, Houston, Texas

The magnitude, variance, and directionality of the velocity perturbations of the fragments of a satellite can provide information regarding the nature and intensity of breakup. It has significant bearing on the distribution of debris around the Earth and is needed for the modeling of the debris environment in low-Earth orbit. The standard method of calculating the velocity perturbations from a fragmentation event is based on the rendezvous equations. This method, however, fails in many of the observed breakups. This paper describes a method of calculating the three orthogonal components of the velocity change using three simultaneous equations provided by the changes in specific energy, specific angular momentum, and plane orientation of the fragments. The method, based on first principles, does not suffer from the deficiencies of the earlier technique. With this method, the velocity perturbations of the fragments from 20 major satellite fragmentation events have been calculated. This information, together with a recent technique of determining the masses of the fragments, provides a description of the breakup process. It has been found that for the Delta rocket booster class of breakups, the velocity distribution can be fitted to a beta function. There is a general negative correlation between the mass and the velocity change of the fragment. A similar negative correlation exists between the effective diameter as measured by the radar cross section, and the velocity change. The angular distributions of the observed debris have been obtained, which can aid in the interpretation and categorization of the cause of breakup.

Introduction

ONE of the fundamental quantities in satellite fragmentation events is the velocity change suffered by a fragment. The magnitudes of these velocity changes may be used as indicators of the type of breakup.[1] The directionality of the velocity perturbations may give clues as to the nature and intensity of the explosion.[2] The traditional method of calculating these velocity changes is based on inverting the equations of the changes in the orbital element sets due to velocity perturbations.[3] This method has been used widely.[4-6] Tan[6] showed that the calculated radial component of the velocity change becomes exceedingly large when either the parent satellite's orbit was nearly circular or the fragmentation took place near the apsidal points. Similarly, the cross-range component of the velocity change becomes singular when the argument of latitude was 90° or 270°. As a number of breakups fall into these categories, this technique frequently fails to give the correct answers. In fact, the three orthogonal velocity components can be obtained more easily by solving the three simultaneous equations provided by the changes in specific energy, specific angular momentum, and plane orientation. This technique is described in this paper. It is free of the singularities inherent in the Meirovitch[3] approach. Both of these techniques assume that the orbital element sets are consistent with the point of breakup, the position of which is assumed to be known.

Received Jan. 20, 1989; revision received July 8, 1989.

*Senior Scientist.
†Summer Faculty; also, Associate Professor, Department of Physics, Alabama A&M University, Normal, AL.

Method

To calculate the velocity perturbations imparted to the fragments, it is convenient to use the parent satellite's local frame of reference at the point of breakup.[7,8] The three orthogonal directions are then defined by the radial and down-range directions in the plane of the orbit and the cross-range direction perpendicular to the plane of the orbit and along the angular momentum vector (Fig. 1). In this coordinate system, the velocity vector v of the parent has the components v_r, v_d, and 0. From astrodynamics,

$$v = \{\mu[(2/r) - (1/a)]\}^{1/2} \tag{1}$$

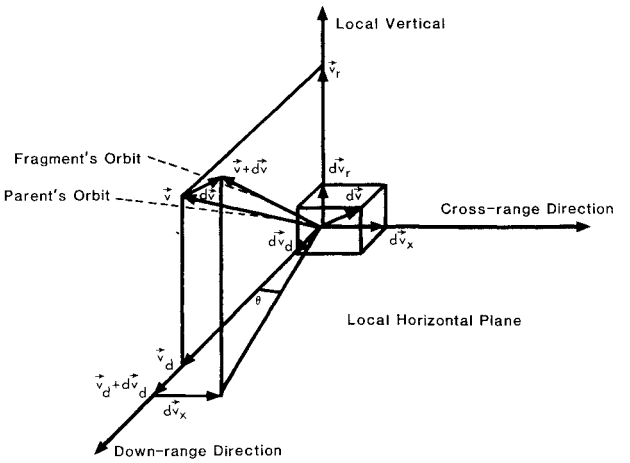

Fig. 1 Local reference frame showing the velocity components of the parent satellite and the fragment. Solid lines are the projections of velocity and delta velocity on the three axes.

$$v_d = \{\mu a[(1-e^2)/r^2]\}^{1/2} \quad (2)$$

$$v_r = \pm\{v^2 - v_d{}^2\}^{1/2} \quad (3)$$

where a is the semimajor axis, e the eccentricity of the parent's orbit, r the radial distance to the breakup point, and μ the gravitational parameter. In Eq. (3), the plus sign corresponds to the ascending mode of the satellite (true anomaly $\nu < 180$ deg), whereas the minus sign corresponds to the descending mode ($\nu > 180$ deg).

Upon fragmentation, the velocity of a fragment v' will have the components $v_r + dv_r$, $v_d + dv_d$, and dv_x, where dv_r, dv_d, and dv_x are the velocity perturbations received by the fragment during breakup. In consequence, the fragment would suffer changes in energy, angular momentum, and orbital-plane orientation. The change in specific energy is given by

$$E' - E = (1/2)(v'^2 - v^2) = -(\mu/2)[(1/a') - (1/a)] \quad (4a)$$

or

$$1/2[(v_r + dv_r)^2 + (v_d + dv_d)^2 + dv_x{}^2 - v_r{}^2 - v_d{}^2]$$

$$= -(\mu/2)[(1/a') - (1/a)] \quad (4b)$$

where a' is the semimajor axis of the fragment's orbit. Similarly, if e' is the eccentricity of the fragment's orbit, the change in specific angular momentum is given by

$$h'^2 - h^2 = |r \times v'|^2 - |r \times v|^2 = \mu a'(1-e'^2)$$

$$-\mu a(1-e^2) \quad (5a)$$

or

$$r^2[(v_d + dv_d)^2 + dv_x^2 - v_d^2] = \mu a'(1-e'^2) - \mu a(-e^2) \quad (5b)$$

Finally, the plane-change angle ζ of the perturbed orbit from the unperturbed orbit is given by (Fig. 2)

$$\tan\zeta = \frac{dv_x}{v_d + dv_d} \quad (6)$$

Equations (4–6) comprise three simultaneous equations that can be solved for three unknowns: dv_r, dv_d, and dv_x. The solution is given by

$$dv_r = \pm\{\mu[(2/r) - (1/a')] - (\mu/r^2)a'(1-e'^2)\}^{1/2} - v_r \quad (7)$$

$$dv_d = (\cos\zeta/r)[\mu a'(1-e'^2)]^{1/2} - v_d \quad (8)$$

$$dv_x = (\sin\zeta/r)[\mu a'(1-e'^2)]^{1/2} \quad (9)$$

These equations can be shown to be equivalent to Eqs. 14, 16,and 17 of Ref. 8. In Eq. (7), the plus sign corresponds to the ascending mode of the fragment orbit (true anomaly $\nu' < 180$ deg), whereas the minus sign corresponds to the descending mode ($\nu' > 180$ deg). Only the positive square sign of the square root in Eqs. (8) and (9) is retained. Equations (7–9) thus provide the three orthogonal components of the velocity change from a knowledge of the orbital elements of the original satellite and fragment.

The plane-change angle ζ can be expressed as a function of the inclinations i and i' of the parent's and the fragment's orbits, respectively, and λ, the latitude of the breakup point.[9] Applying the cosine law to the spherical triangle $AA'B$ of Fig. 2 and the sine law to the triangle ABC and $A'BC$, one obtains

$$\zeta = \pm\cos^{-1}\frac{\cos i\cos i' + \sqrt{(\cos^2\lambda - \cos^2 i)(\cos^2\lambda - \cos^2 i')}}{\cos^2\lambda} \quad (10)$$

Here, the plus sign corresponds to $i' > i$ and the minus sign corresponds to $i' < i$ on northbound orbits with the opposite sense on southbound orbits. This corresponds to a positive plane-change angle corresponding to positive rotation about the x axis in the local reference frame previously described.

The true anomaly ν' of the fragment at the time of breakup, which determines the sign of $v_r + dv_r$ in Eq. (7), is determined from the argument of latitude u' and the argument of perigee ω' of the fragment at the time of breakup as

$$\nu' = u' - \omega' \quad (11)$$

Applying the sine law to the spherical triangle $A'BC$ of Fig. 2, one obtains

$$u' = \sin^{-1}(\sin\lambda/\sin i') \quad (12a)$$

or

$$u' = 180 - \sin^{-1}(\sin\lambda/\sin i') \quad (12b)$$

where the first solution corresponds to the northbound motion of the fragment and the second to the southbound motion at the time of breakup. Since the argument of the perigee is perturbed by the oblateness of the Earth, the argument of perigee of the fragment at the time of observation ω_o' is different from its value at the time of fragmentation ω'. From the rate of precession derived by King-Hele,[10] one obtains

$$\omega' = \omega_o' - \frac{4.98(5\cos^2 i' - 1)\Delta t}{(a'/r_o)^{7/2}(1-e'^2)^2} \quad (13)$$

where Δt is the time of observation from the time of fragmentation. Here, ω' and ω_o' are expressed in degrees and Δt in days. It was verified from successive United States Space Command (USSPACECOM) data sets that the true anomaly predicted using Eq. (13) was generally accurate to within about 2 deg/yr for all types of low Earth orbits. Thus, this method can be used satisfactorily to calculate the initial true anomaly, as this information is needed only to unambiguously determine the sign of the radial velocity perturbation.

To calculate the velocity perturbation, the orbital elements of satellite fragments for several breakups were obtained from USSPACECOM historical data. The orbital elements of the fragmented satellites as well as the coordinates at the time of breakup were taken from the catalog of Johnson and Nauer.[11] It should be noted that the information about the point of breakup may not be accurate in many instances. The point of breakup is not always deserved by the USSPACECOM sensors, and, thus, information has to be derived from a few fragments seen immediately following breakup. For breakups early in the space program and in particular Soviet breakups, this problem is quite serious and did not allow analysis of these breakups.

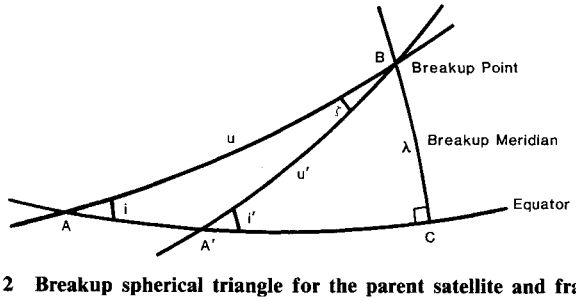

Fig. 2 Breakup spherical triangle for the parent satellite and fragment.

To calculate the velocity perturbation immediately following breakup, the orbital elements of the fragments have to be obtained at that time. In general, this is not practical and the data become available many months or even years following breakup. In such an event, atmospheric drag causes the orbits to lose energy and circularize. This drag effectively causes velocity perturbations of its own and thus masks the velocity perturbation due to breakup. To calculate the orbital elements of the cataloged debris at the time of breakup, a knowledge of the area-to-mass ratio of the fragment is needed. With a technique developed earlier,[12] the area-to-mass ratio of these fragments is obtained from the decay in the apogee and perigee altitudes as a function of time due to atmospheric drag. By using the same propagation model, the calculated area to mass, the apogee and perigee heights are determined at the time of breakup from the very first observation immediately following breakup. The disadvantage of this technique is that only those fragments for which there are at least three orbital element sets can be analyzed.

By using the "corrected" orbital elements at the time of breakup, the coordinates of the point of breakup, and the orbital elements of the parent satellite, the velocity perturbations of 20 satellite breakups have been calculated. The results are presented in the next section. In interpreting these results, it should be realized that the inaccuracies of the input data from the USSPACECOM system and the point of breakup are not truly known. However, it is expected that the orbital element sets from this system are fairly accurate.

Results

Breakup of Solwind

The results from velocity perturbation calculations can perhaps be illustrated best using the breakup of P-78 (Solwind). This is the only breakup definitely known to be caused by a hypervelocity collision of two satellites. The reason for choosing this breakup is that there are two data sets, one taken almost immediately following the breakup and the second (USSPACECOM element sets) acquired over a considerable length of time. This allows one to look at the calculated velocities from the near-time data taken by the U.S. Air Force Cavalier phased-array radar and compare them to the velocities from "undecayed" USSPACECOM element sets. As the early data set is a snapshot at a single time, one cannot calculate the area-to-mass ratio and derive the masses of these fragments. Also, these objects cannot be correlated to the subsequent USSPACECOM cataloged data.

Figure 3 includes scatter plots of the dv_r against dv_d and of dv_d vs dv_x for the data immediately following breakup. These data show that there were three objects (+) that carried a large negative component of the radial velocity, a large negative component of the cross-range velocity, and a large positive component of the down-range velocity compared to the rest of the fragments. These two figures also indicate that a small fraction of these objects had very nearly the same velocity as the original satellite. These are objects with essentially zero values of dv_r, dv_d, and dv_x and are indicated by the string of horizontal asterisks near zero values. The mean values of dv_r, dv_d, and dv_x are found to be -17.6, -4.9, and 22.5 m/s; that is, the mean values are not zero. If one *assumes* that the direction of the momentum vector is the same as that of the velocity vector, one finds a net momentum transfer in the direction of colatitude $[\cos^{-1}(dv_r/dv)]$ of 103.1°, that is, 13.1° below the local horizontal, and longitude $[\tan^{-1}(dv_x/dv_d)]$ of 102.3°, that is, at an angle of 102.3° to the velocity vector in the local horizontal plane. This implies that the smaller interceptor mass of 15.9 kg[13] arrived from the direction of approximately 76.9° colatitude (13.1° above the local horizontal) and −77.7° longitude (77.7° right of the down range for an observer looking heads-up down the velocity vector) to hit a larger mass of 853.7 kg Figure 4 gives the frequency distribution of the velocity components in this collision. Ex-

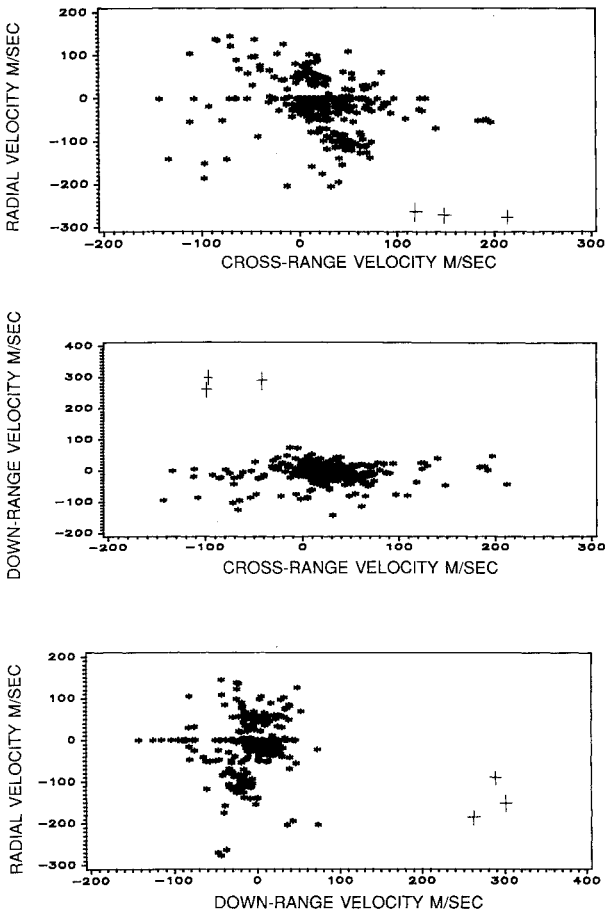

Fig. 3 Breakup of P-78 (Solwind) calculated with the data very soon after breakup; dv_r vs dv_d and dv_d vs dv_x.

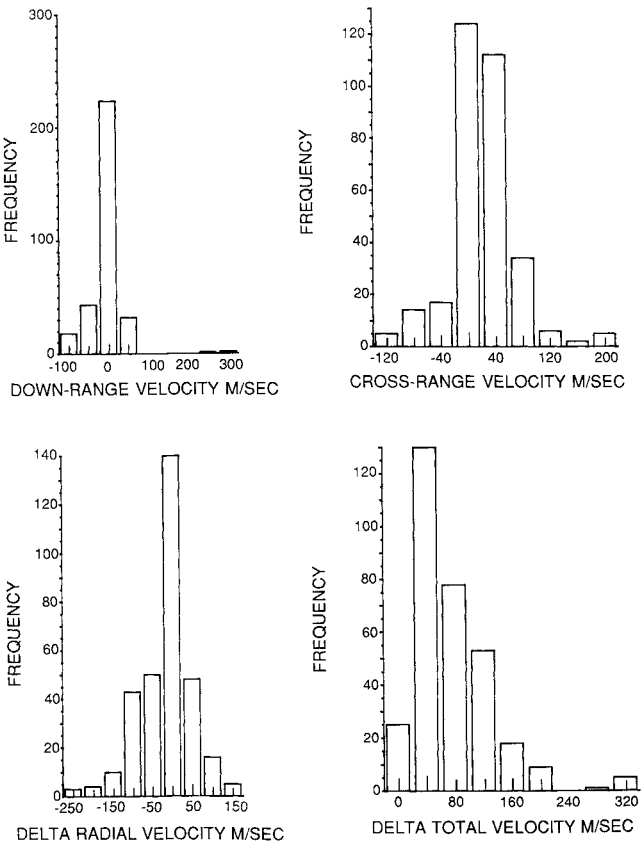

Fig. 4 Solwind fragment velocity components for the data in Fig. 3.

cept for three pieces, indicated by + in Fig. 3, with large velocity perturbations, the distributions are nearly symmetric but not quite centered on zero, indicating the preferred direction of the debris fragments.

The analysis of the cataloged pieces (about one-half the number seen by the Cavalier phased-array radar) is shown in Fig. 5. The frequency histogram now shows that a large fraction of fragments with negative down-range velocity are missing from the distribution. A simple calculation indicates that a 1.7% decrease in down-range velocity would have been sufficient to deorbit these fragments. These results are completely consistent with this calculation. As the time history of these fragment element sets is known, the masses of these fragments can be calculated.[12] With this knowledge of the masses, the momentum transfer can be calculated. These results indicate that the net transfer is in the direction given by a colatitude of 91.1° and longitude of 91.8°, almost the same as the velocity direction from the Cavalier data. Hence, the analysis of the direction of the incoming satellite just derived should be close to the correct value. Thus, this method of deriving velocity perturbations can be used for reconstructing the encounter conditions for collisional breakup orbits.

The Solwind breakup data also can be used to provide information on the velocity distribution function of the debris fragments as a function of the size (or mass). Su and Kessler[14] have suggested a relation of the form

$$\log(v/v_p) = a + b\log(d/d_{\max}) + c\log^2(d/d_{\max}) \qquad (14)$$

where v_p is the projectile velocity; v is the velocity of the debris fragment of diameter d; and a, b, c, and $d_{\max}$ are constants. Figure 6 shows a plot of the velocity vs the effective diameter of the debris fragments. The diameter is derived from the average Cavalier radar cross-section data. Although there is an indication that the Cavalier data have a bias compared to the Eglin radar cross-section data,[5] is is not considered here. This only will affect the values of the coefficients but not the form

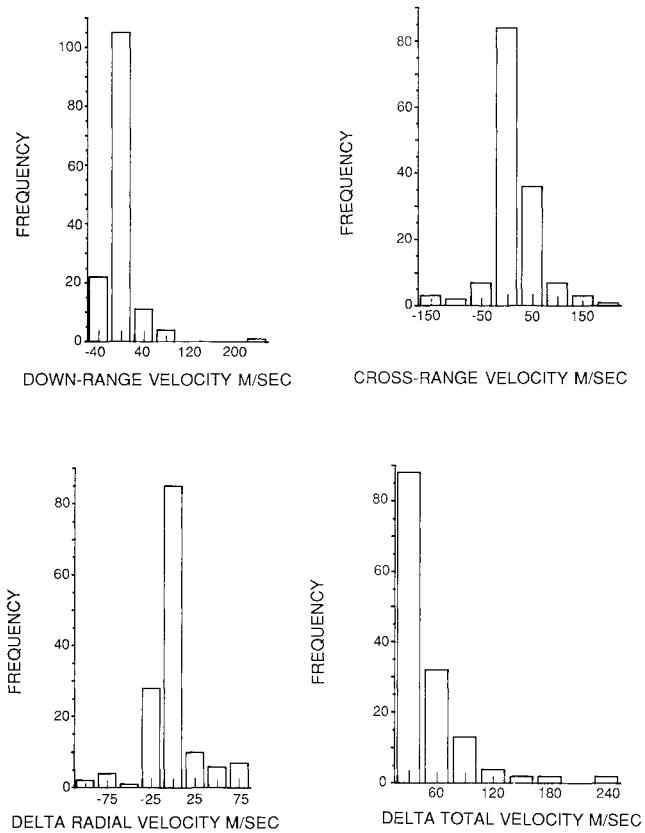

Fig. 5 Solwind fragment velocity components derived from US-SPACECOM cataloged data.

of Eq. (14). The solid line is the fit to the model of Eq. (14) and indicates that the model fits the data well. A simple power law relationship would also fit this data well. If we absorb $d_{\max}$ in coefficients b and c, the fit results are $a = 1.6712$, $b = -0.2966$, and $c = 1.6856$. These coefficients are quite different from those obtained by Su.[15] The reason for that is that Su was concerned more with smaller-size objects and maintained a constant velocity below about 1 μm size objects; our coefficients are valid only over the size range of 15 to 90 cm.

Another related question that can be studied using the Solwind breakup data is the velocity distribution function, that is, the spread around the most probable value predicted by Eq. (14). In the model developed by Su[15] and Kessler et al.,[16] it is assumed that the velocity distribution goes linearly to zero at $0.1v$ and $1.3v$. This implies that maximum velocity perturbation is 1.3 times the most probable value. Figure 7 is the differential velocity distribution of all fragments seen in this collision and indicates that the most probable value is around 60 m/s, but the maximum extends to 360 m/s, six times the maximum value. This distribution can be fitted to a beta function

$$\frac{dN}{dv} = A\left(\frac{v}{v_{\max}}\right)^{\alpha-1}\left(\frac{1-v}{v_{\max}}\right)^{\beta-1} \qquad (15)$$

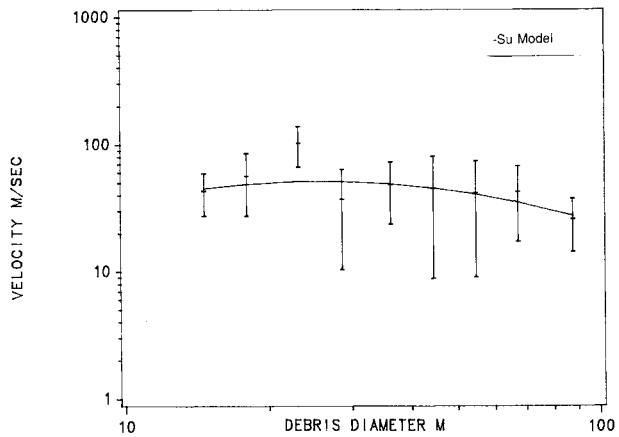

Fig. 6 Average velocity change, immediately following the breakup of Solwind, vs the diameter of the fragments.

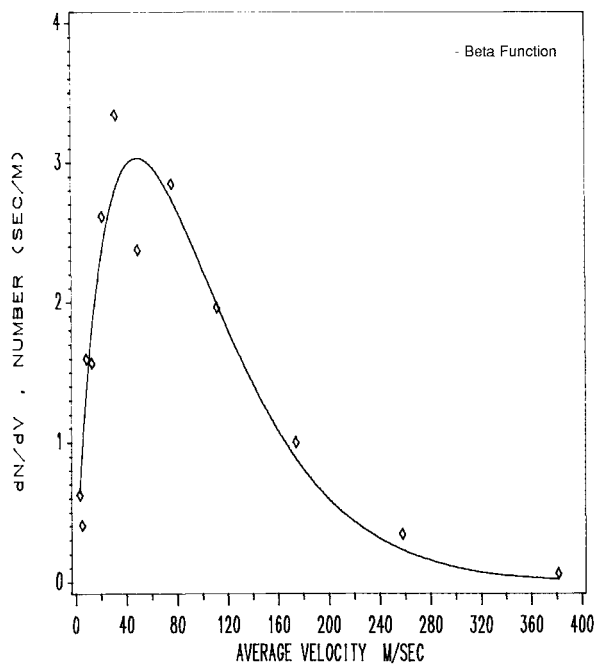

Fig. 7 The differential velocity distributions, dN/dv, vs the average velocity change irrespective of the size.

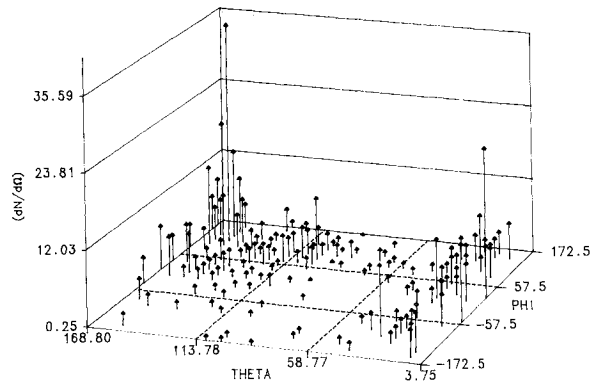

Fig. 8 Angular distribution, $dN/d\Omega$, vs the colatitude θ and azimuth ϕ for the Solwind breakup.

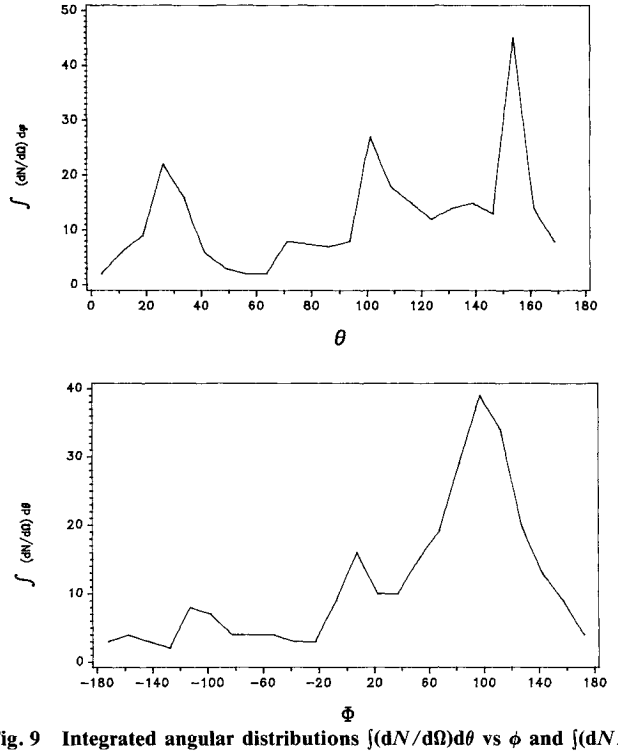

Fig. 9 Integrated angular distributions $\int(dN/d\Omega)d\theta$ vs ϕ and $\int(dN/d\Omega)d\phi$ vs θ for the Solwind breakup.

where A, α, and β are constants. An examination of the distribution function as a function of diameter shows that the maximum value of the velocity, at any diameter, is more than 1.3 times the most probable value. If this spreading function holds at lower sizes also, then the debris flux models[16] will yield significantly different results than currently postulated.

The angular distribution of fragments in the Solwind breakup is another potentially important attribute of breakup. Benz et al.[2] have pointed out that the angular distribution of fragments as they emerge from a breakup may be an indicator of the type of breakup. They have suggested various kinds of breakup patterns, such as the clam model, half-segment model, and the octant model that results from various tank failure modes. The PISCES[1,2] code predicted the range of velocity of the fragments. The model, however, does not produce a velocity distribution. Although this model is not applicable to a hypervelocity collision, the idea of looking at the angular distribution is equally valid here. If we define the elementary solid angle as $d\Omega = \sin\theta\, d\theta\, d\phi$, where θ is the angle between the radial velocity component and the velocity vector, and ϕ is the angle between the cross-range and down-range velocity components, then the angular distribution, $dN/d\Omega$, is defined as the number of fragments per unit solid angle. This is clearly a function of θ and ϕ. Figure 8 is a plot of $dN/d\Omega$ as a function of θ and ϕ. There is a rather pronounced peak around $\theta = 155$ deg and $\phi = 100$ deg. The distribution is definitely not isotropic. Figure 9 is a plot of $\int(dN/d\Omega)d\phi$ and $\int(dN/d\Omega)d\theta$ as a function of θ and ϕ. They indicate three preferential directions with the main peak around (150, 100 deg) and two smaller peaks around (100, 10 deg) and (28, −110 deg), respectively.

Breakup of Delta-Class Vehicles

Many of the propellant tanks used in the United States Delta second stage have ruptured, leading to a significant source of manmade debris in space. In both modeling the current debris environment and taking corrective action to reduce the chances of these breakups, it is important to understand the causes that lead to these tank failures. The analysis of the velocity pattern can provide some clues toward this end.

Figure 10 is a frequency histogram of the components of the velocity perturbation for the breakup of the second stage used to launch Landsat-1. Note that the frequency distributions are nearly symmetric about zero. Figure 11 shows the angular distribution of these fragments. This pattern is characterized by most of the objects in one hemisphere and only a few in the other hemisphere to conserve the momentum. There appears to be an axis of symmetry that might be the place of rupture itself. This single clam shape is expected based on the analysis of Benz et al.[2] Integrating over the azimuthal and zenith angles, respectively, clearly shows pronounced peaks at about $\theta = 90$ deg and $\phi = -60$ deg. The velocity range of these fragments is from 7 to 381 m/s and is somewhat lower than the predictions of Benz et al.[2] of 15 to 510 m/s for a 0.002-m thick tank. Analysis of the breakup of the Delta second stage used to launch Landsat-2 and Landsat-3 shows that the breakup pattern is nearly identical to that of Landsat-1, but the symmetry axis is not quite the same. The velocity ranges are 28–345 m/s and 28–741 m/s, respectively. These values are in reasonable agreement with the work of Benz et al.[2] for a clam model using the PISCES code.

The National Oceanic and Atmospheric Administration (NOAA) satellites were also launched on a Delta-class vehicle but with different initial conditions. For example, the liquid propellant was 133 kg compared with 88 kg for Landsats. The general breakup pattern was similar to that of Landsats. However, the range of velocities was 9–487 m/s. Although the range is similar to that of Landsat, the maximum velocity was somewhat larger. Benz et al.[2] have offered several explanations for this behavior, but they cannot be verified using these data.

Breakup of Ariane V16 Third Stage

The Spot-Viking (Arianespace) breakup in 1986 was one of the most prolific in terms of the number of debris fragments generated. The cause of this breakup is now known.[2,9,17] Figure 12 shows the velocity distribution from this breakup. The velocity range is from 1.3 to 267 m/s. The angular distribution (Fig. 13) from this breakup, however, shows three well-defined peaks. This distribution is quite different from that seen in the case of Landsat or NOAA breakups and indicates a different breakup mechanism for the two cases.

It was pointed out earlier that the velocity distribution as a function of the debris size (as inferred from the radar cross section) could be written as Eq. (14). This expression provided a satisfactory fit to the P-78 data. Figure 14 gives the results of fitting the combined Delta class of breakups (Landsat's and NOAA's) and the Spot-Viking data. The results of the fit are

Delta class:

$$\log_e v = 3.91 - 0.1008 \log_e d + 0.5774 (\log_e d)^2$$

Spot-Viking:

$$\log_e v = 4.54 - 0.1006 \log_e d + 0.2443 (\log_e d)^2$$

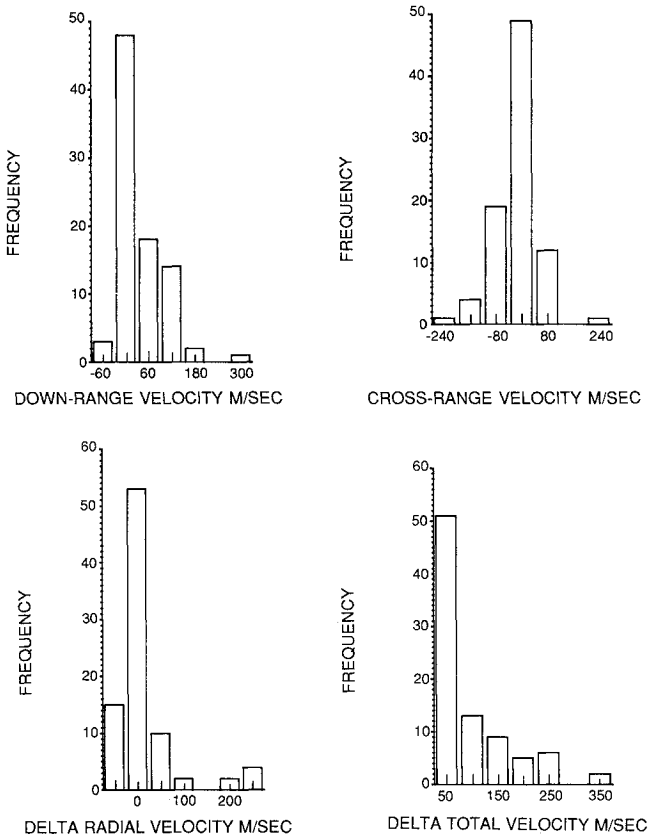

Fig. 10 Frequency distribution of the velocity components in the breakup of Landsat-1, a Delta-class booster.

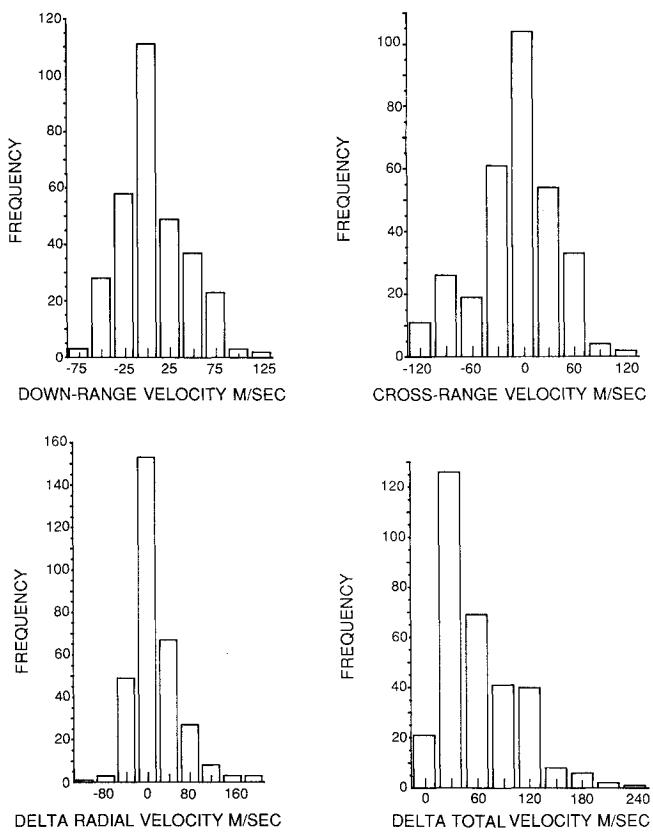

Fig. 12 Frequency distribution of the velocity changes for the Spot-Viking (Arianespace) breakup.

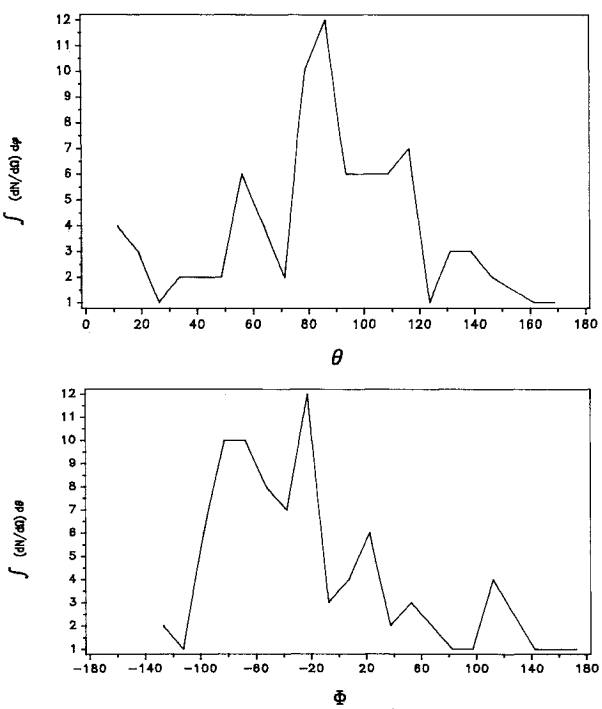

Fig. 11 Integrated angular distribution $\int(dN/d\Omega)d\theta$ vs ϕ and $\int(dN/\Omega)d\phi$ vs θ for Landsat-1 breakup.

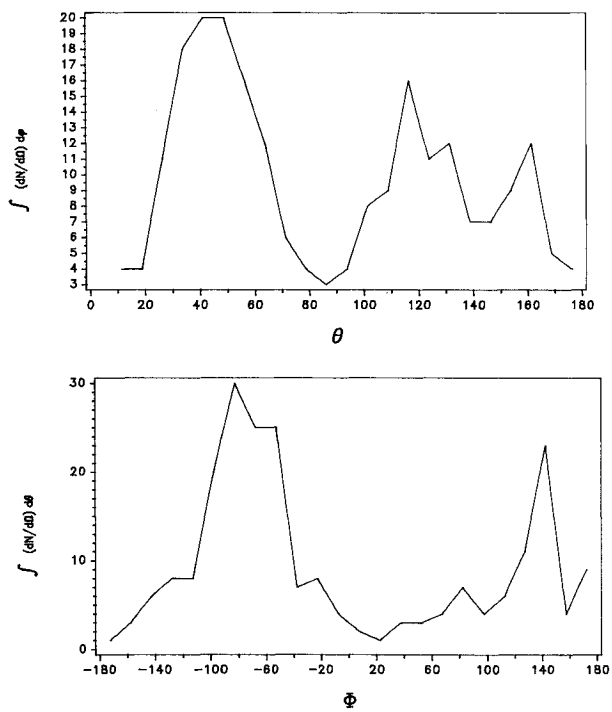

Fig. 13 Integrated angular distribution for the Spot-Viking breakup.

Solwind:

$$\log_e v = 1.67 - 0.2966 \log_e d + 1.686 (\log_e d)^2$$

The velocity for a given diameter is the smallest for the P-78 hypervelocity collision, and roughly the same for the Delta and Spot-Viking breakup. It should be remembered that NOAA's satellite breakups gave slightly higher velocities than Landsat's satellite breakups.

The velocity distribution functions again can be represented by a beta function [Eq. 15] for most of the breakups. In general, the distribution function is broader for Delta compared to Spot-Viking. The distribution function of Soviet high-intensity explosions is characterized by a very small range of velocities (1.3-65 m/s) and is rather narrow. Thus, it is quite

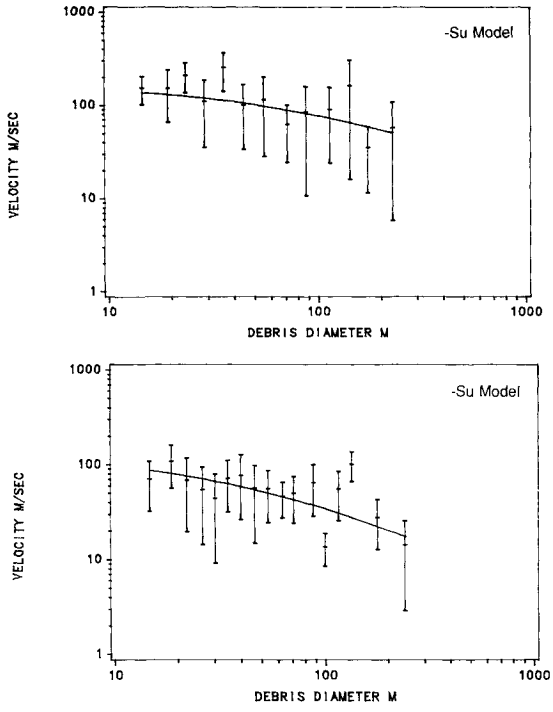

Fig. 14 Differential velocity distribution, dN/dv, for all of the Delta-class rocket booster failures and the Spot-Viking breakup.

clear that not only the velocity-diameter relationship but the velocity distributions itself is different for various classes of breakups. Future debris population models should consider these.

With the knowledge of mass values calculated using the decay in apogee and perigee, the relationship between the mass and velocity and momentum distribution functions can be examined. There is a general decrease of velocity with mass. The cumulative distribution of momentum p can be fitted to an equation of the form $A(p+b)^{-c}$, where A, b, and c are constants.

Conclusions

An analytic technique has been developed that allows one to calculate the velocity perturbation of debris fragments in the breakup of a satellite using the orbital element sets and knowing the position of the breakup. This technique does not suffer from the deficiencies of many of the early techniques. With this technique and the knowledge of the mass of the fragments, the direction of the incoming satellite in the hypervelocity collision of P-78 has been determined. It has been shown that the angular distribution of the debris from three Delta second-stage Landsat breakups is essentially the same as is the total velocity change. This indicates the common origin of these breakups. The velocity range is slightly higher for NOAA breakups, although these were also Delta rocket-booster breakups. The angular distribution for Spot-Viking is significantly different than that for Delta second-stage breakups and the P-78 collision although the velocity range is not too different from that for the Delta second-stage breakups. The velocity-diameter relationship observed from these breakups is consistent with that derived from the laboratory hypervelocity collision experiment, but other formulations, such as a power-law fit, cannot be ruled out. The coefficient of the fit depends on the nature of the breakup. For debris size (>15 cm), the velocity distribution can be fitted to a beta function and shows a much larger range of velocities than used earlier. This function is dependent on the nature of the breakup and may depend on size also. The results show, as expected, a general decrease of velocity with debris mass.

Acknowledgment

We appreciate the help of Philip Anz-Meador of Lockheed Engineering & Science Company in generating the data sets used in this analysis and numerous discussions. We would also like to thank Donald Kessler and Andrew Potter for general discussions about the applicability of this work to various orbital debris models.

References

[1]Eck, M., and Mukunda, M., "Predicting the Velocity and Azimuth of Fragments Generated by the Range Destruction or Random Failure of Rocket Casings and Tankage," 39th Congress of the International Astronautical Federation, Paper IAF-88-523, Bangalore, India, 1988.

[2]Benz, F. J., Bishop, C. V., and Eck, M. B., "Explosive Fragmentation of Orbiting Propellent Tanks," *Proceedings of the Upper Stage Breakup Conference*, Houston, TX, May 1987.

[3]Meirovitch, L., *Methods of Analytical Dynamics*, McGraw-Hill, New York, 1970, pp. 453–456.

[4]McKnight, D. S., "Discerning the Cause of Satellite Breakups," 62nd Annual AAS Meeting, Boulder, CO, 1986.

[5]Kling, R., "Postmortem of a Hypervelocity Impact," Teledyne Brown Engineering, Rept. CS86-LKD-001, 1986.

[6]Tan, A., "Analysis and Interpretation of Satellite Fragmentation Data," edited by W. B. Jones and S. H. Golstein, NASA CR 172009, 1987.

[7]Wiesel, W., "Fragmentation of Asteroids and Artificial Satellites in Orbit," *ICARUS*, Vol. 34, 1978, pp. 99–116.

[8]Reynolds, R. C., "Evolution of Debris Cloud Immediately After a Satellite Breakup in Orbit," Lockheed Engineering & Science Co., Houston, TX, 1988.

[9]Badhwar, G. D., Potter, A. E., Anz-Meador, P. D., and Reynolds, R. C., "Characteristics of Satellite Breakups from Radar Cross-Section and Plane Change Angle," *Journal of Spacecraft and Rockets*, Vol. 25, No. 6, 1988, pp. 420–426.

[10]King-Hele, D., *Theory of Satellite Orbits in an Atmosphere*, Butterworths, London, 1964, p. 4.

[11]Johnson, N. L., and Nauer, D. J., "History of On-Orbit Satellite Fragmentations," Teledyne Brown Engineering, Rept. CS88-LKD-001, 1987.

[12]Badhwar, G. D., and Anz-Meador, P. D., "Determination of the Area and Mass Distribution of Orbital Debris Fragments," *Earth, Moon, and Planets*, 1989.

[13]Robinson, C. A., Jr., "USAF Will Begin Anti-Satellite Testing," *Aviation Week and Space Technology*, Dec. 19, 1983, pp. 20–22.

[14]Su, S.-Y. and Kessler, D. J., "Time Evolution of the Near-Earth Man-Made Orbital Debris Environment," Lockheed Engineering & Science Co., Houston, TX, Rept. LESC-26316, 1984.

[15]Su, S.-Y, "On the Velocity Distribution of Collisional Fragments in the New Ejecta Model and Its Effect on Future Debris Environment," Lockheed Engineering & Science Co., Houston, TX, July 1986.

[16]Kessler, D. J., Reynolds, R. C., and Anz-Meador, P.D., "Orbital Debris Environment for Spacecraft Designed to Operate in Low Earth Orbit," NASA TM 100-471, April 1989.

[17]Cour-Palais, B. G., and Crews, J. E., "Hypervelocity Impact and Upper Stage Breakups," Upper Stage Breakup Conference, Houston, TX, May 1987.